Effects of Lithium Doping on the Polymer Chain Dynamics in Siloxane/Poly(Ethylene Oxide) Ormolyte Nanocomposites: A ^{13}C and ^{7}Li Exchange Solid-State NMR Study

André L. B. S. Bathista,[†] Eduardo R. deAzevedo,[†] Antonio C. Bloise,[†] Karim Dahmouche,[‡] Patrick Judeinstein,[§] and Tito J. Bonagamba*,[†]

Instituto de Física de São Carlos, Universidade de São Paulo, Caixa Postal 369, CEP: 13560-970, São Carlos-SP, Brazil, Universidade Estadual da Zona Oeste, Campo Grande 23070-200, Rio de Janeiro-RJ, Brazil, and RMN en Milieu Orienté, ICMM, (UMR CNRS 8182), Bâtiment 410, Université Paris Sud, Orsay, France

Received March 31, 2006. Revised Manuscript Received January 30, 2007

^{7}Li and ^{13}C solid-state NMR methods were used to study Li^{+}-doped siloxane/poly(ethylene oxide) hybrid electrolyte materials, where the polymer chains are linked to the inorganic phase through covalent bonds. These methods were employed to analyze the effects of the interactions between the organic and inorganic (siloxane and lithium) phases on the polymer dynamics. The motion geometry of polymer chains was found to be very similar for Li^{+}-doped and non-doped Ormolytes. However, a significant effect of the Li^{+} doping on the non-exponentiality of the correlation time functions that describe the polymer chain dynamics was observed, and a model that supports such behavior was proposed.

Introduction

The combination of the appropriate processing conditions with the adequate choice of the organic and inorganic components dictates the morphology, molecular structure, and properties of hybrid materials. The intense activity in this domain of research is due to the extraordinary implications that derive from the possibility of combining multifunctional advanced compounds by mixing, at the nanosize level and in a single material, organic and inorganic components. The hybrid material concept seems to be particularly well adapted for the preparation of advanced solid polymer electrolytes presenting ion-conducting properties, with the advantage of replacing viscous liquid systems by solid or rubbery materials.[1−3]

For the preparation of solid polymer electrolytes, lithium salt (such as perchlorate or triflate) is dissolved inside the organic phase of the hybrid matrices, leading to materials with reasonable ionic conductivity (1×10^{-6} to 1×10^{-4} S/cm).[4−6] Among the various systems that have been proposed in the last years, the family of versatile compounds classified as diureasils, in which polyether-based chains are grafted on both ends to a siliceous backbone through urea functionalities, is noteworthy. The denomination given for these materials is ormolytes.[1−3] When doped with Li salts, these solid, transparent, and flexible nanocomposites exhibit a reasonable ionic conductivity at room temperature ($\sim 1 \times 10^{-6}$ S/cm).[4−6] Because of the presence of covalent bonds between the inorganic and organic phases (Type II ormolytes), these materials result in a cross-linked polymer network and exhibit good chemical stability and mechanical properties.[2−8]

For understanding the polymer dynamics inside these hybrids, we employed several solid-state NMR methods.[4−6,9−14] It was found that the ionic mobility is assisted by the polymer chain motion, which depends on the chain length, Li^{+} doping level, and the type of hybrid material.[9,10] Additional information about the chain dynamics in the slow-motion regime (milliseconds to seconds) was obtained using solid-state 1D and 2D exchange NMR experiments.[11,12] For non-doped Type II ormolytes at temperatures around the glass-transition temperature, it was shown that the polymer segments near

* To whom correspondence should be addressed. E-mail: tito@if.sc.usp.br.
[†] Universidade de São Paulo.
[‡] Universidade Estadual da Zona Oeste.
[§] RMN en Milieu Orienté.

(1) Ravaine, D.; Seminel, A.; Charbouillot, Y.; Vincens, M. *J. Non-Cryst. Solids* **1986**, *82*, 210−219.
(2) Judeinstein, P.; Brik, M. E.; Bayle, J. P.; Courtieu, J.; Rault, J. *Mater. Res. Soc. Symp. Proc.* **1994**, *346*, 937−942.
(3) Brik, M. E.; Titman, J. J.; Bayle, J. P.; Judeinstein, P. *J. Polym. Sci., Part B: Polym. Phys.* **1996**, *34*, 2533−2542.
(4) Dahmouche, K.; Atik, M.; Mello, N. C.; Bonagamba, T. J.; Panepucci, H.; Aegerter, M. A.; Judeinstein, P. *Mater. Res. Soc. Symp. Proc.* **1996**, *435*, 363−368.
(5) Dahmouche, K.; Atik, M.; Mello, N. C.; Bonagamba, T. J.; Panepucci, H.; Aegerter, M. A.; Judeinstein, P. *J. Sol−Gel Sci. Technol.* **1997**, *8*, 711−715.
(6) Dahmouche, K.; Atik, M.; Mello, N. C.; Bonagamba, T. J.; Panepucci, H.; Judeinstein, P.; Aegerter, M. A. *Sol. Energy Mater. Sol. Cells* **1998**, *54*, 1.
(7) Lesot, P.; Chapuis, S.; Bayle, J. P.; Rault, J.; Lafontaine, E.; Campero, A.; Judeinstein, P. *J. Mater. Chem.* **1998**, *8*, 147−151.
(8) Gomes Correia, S. M.; V, d. Z. B.; Silva, M. M.; Barros, S.; Sa'Ferreira, R. A.; Carlos, L.; Passos de Almeida, A. P.; Smith, M. J. *Solid State Ionics* **2003**, 85−93.
(9) Mello, N. C.; Bonagamba, T. J.; Panepucci, H.; Dahmouche, K.; Judeinstein, P.; Aegerter, M, A. *Macromolecules* **2000**, *33*, 1280−1288.
(10) de Souza, P. H.; Bianchi, R. F.; Dahmouche, K.; Judeinstein, P.; Faria, R. M.; Bonagamba, T. J. *Chem. Mater.* **2001**, *13*, 3685−3692.
(11) deAzevedo, E. R.; Reichert, D.; Vidoto, E. L. G.; Dahmouche, K.; Judeinstein, P.; Bonagamba, T. J. *Chem. Mater.* **2003**, *15*, 2070−2078.
(12) Yang, D. K.; Zax, D. B. *Solid State Nucl. Magn. Reson.* **2006**, *29*, 153−162.
(13) Joo, C. G.; Bronstein, L. M.; Karlinsey, R. L.; Zwanziger, J. W. *Solid State Nucl. Magn. Reson.* **2002**, *22*, 235−246.
(14) Kao, H. M.; Chao, S. W.; Chang, P. C. *Macromolecules* **2006**, *39*, 1029−1040.

10.1021/cm060762e CCC: $37.00 © 2007 American Chemical Society
Published on Web 03/13/2007

the linkage group undergo restricted motions and do not execute large amplitude reorientations. In addition, it was demonstrated that the molecular motion in non-doped Type II ormolytes is more hindered for samples with smaller chain lengths. Therefore, the results revealed that the heterogeneities of the slow molecular motions of the polymer chains depend on the chain length and the nature of the interaction between the organic and inorganic (siliceous backbone) phases. However, the effects of Li^+ doping on the specific characteristics of the chain motion in ormolytes, such as motional geometry and motional correlation functions, have not been studied.

In this work, ^{13}C solid-state exchange NMR experiments[15] and line shape analysis were performed to obtain information about the effects of Li^+ doping on the chain dynamics in Type II ormolytes. To characterize the correlation functions of the molecular motions, in particular its non-exponentiality, we used 1D pure-exchange NMR experiments (1D-PUREX). However, because 1D PUREX is a kind of two-time exchange NMR experiment, it is not capable of elucidating the origin of such non-exponentiality: heterogeneous or homogeneous scenario.[16] However, previous works have shown that the non-exponentiality of the correlation function observed for glass-transition molecular motions are mostly due to dynamical heterogeneities, which can be related to heterogeneities of the molecular microenvironment.[16−19] Besides, the intrinsic heterogeneous character of the ormolytes[3] also favors the presence of heterogeneities rather than intrinsic non-exponentiality as the cause of the non-exponential behavior of the correlation functions. In the specific case of ormolytes, this heterogeneity is predominately due to the presence of the covalent bonds among the polymer ends and the silica structures. This was confirmed by using electron paramagnetic resonance measurements to analyze samples prepared with nitroxide spin probes.[3] Therefore, in this work, we will assume that the non-exponentiality observed for the correlation functions for the motions around the polymer glass transition are due to a distribution of correlation times, but an alternative interpretation based on intrinsic non-heterogeneity can also be done.

^7Li stimulated echo exchange NMR experiments were also performed in order to investigate the cation dynamics in the slow-motion regime. The NMR methods used in this work are effective for studying dynamics in the millisecond to second time scale, which takes place at temperatures around the motional narrowing of the NMR line width that occurs because of the polymer glass transition.[4−6,9,10−11] For this reason, the experiments were carried out at temperatures slightly above the polymer glass transition as determined by differential scanning calorimetry (DSC).

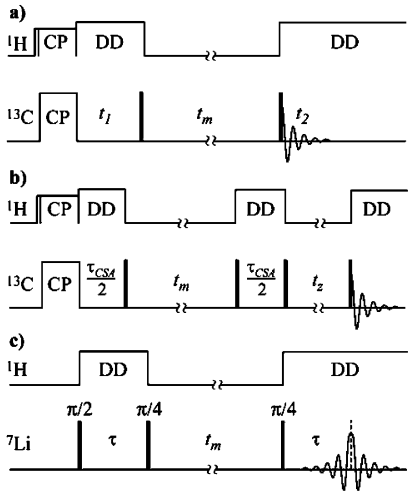

Figure 1. Pulse sequences used in the exchange experiments: (a) 2D exchange; (b) 1D PUREX (90° pulses are filled in black); and (c) stimulated echo experiments with ^1H broadband decoupling (45° pulses are indicated). For all these pulse sequences, phase cycling is applied to eliminate spectral artifacts and select the desirable coherences.

NMR Background

This section gives a short introduction about the exchange methods employed in this work. Detailed descriptions of the methods described below are found in references.[15,20−27]

2D Exchange. Figure 1a shows the pulse sequence used for the static 2D exchange experiment. In this experiment, the orientation-dependent NMR frequencies are monitored before (t_1) and after (t_2) a mixing time (t_m) at which molecular reorientations can occur. If slow molecular reorientations (exchange) do not occur during t_m, the resulting 2D spectrum is purely diagonal. In contrast, if exchange occurs during t_m, off-diagonal intensities are observed. The shape of the 2D spectrum strongly depends on motional amplitude, making it possible to distinguish whether the motion involves small (<20°) or large amplitude reorientations. The identification of the motional amplitude can be made from the 2D spectrum, adopting a suitable model for the motion.[15]

1D Pure Exchange (PUREX). The pulse sequence for the 1D PUREX NMR experiment[24,28] is shown in Figure 1b. One-Dimensional PUREX is a stimulated echo experiment (Jeener−Broekaert experiment[29]) that detects only segments reorienting in the exchange frequency window (hertz to kilohertz). This is achieved by monitoring the signal reduction due to changes in the orientation-dependent chemical-

(15) Schmidt-Rohr, K.; Spiess, H. W. *Multidimensional Solid-State NMR and Polymers*, 1st ed.; Academic Press: London, 1994; Vol. 1.
(16) Schmidt-Rohr, K.; Spiess, H. W. *Phys. Rev. Lett.* **1991**, *66*, 3020−3023.
(17) Vogel, M.; Brinkmann, C.; Eckert, H.; Heuer, A. *Phys. Rev. B* **2004**, *69*.
(18) Tracht, U.; Wilhelm, M.; Heuer, A.; Feng, H.; Schmidt-Rohr, K.; Spiess, H. W. *Phys. Rev. Lett.* **1998**, *81*, 2727−2730.
(19) Tracht, U.; Heuer, A.; Spiess, H. W. *J. Chem. Phys.* **1999**, *111*, 3720−3727.
(20) Jeener, J.; Meier, B. H.; Bachmann, P.; Ernst, R. R. *J. Chem. Phys.* **1979**, *71*, 4546−4553.
(21) Wefing, S.; Spiess, H. W. *J. Chem. Phys.* **1988**, *89*, 1219−1233.
(22) Wefing, S.; Kaufmann, S.; Spiess, H. W. *J. Chem. Phys.* **1988**, *89*, 1234−1244.
(23) Kaufmann, S.; Wefing, S.; Schaefer, D.; Spiess, W. *J. Chem. Phys.* **1990**, *1*, 197−214.
(24) deAzevedo, E. R.; Bonagamba, T. J.; Schmidt-Rohr, K. *J. Magn. Reson.* **2000**, *142*, 86−96.
(25) deAzevedo, E. R.; Hu, W.-H.; Bonagamba, T. J.; Schmidt-Rohr, K. *J. Chem. Phys.* **2000**, *112*, 8988.
(26) Bohmer, R.; Jörq, T.; Qi, F.; Titze, A. *Chem. Phys. Lett.* **2000**, *316*, 419−424.
(27) Qi, F.; Jorg, T.; Bohmer, R. *Solid State Nucl. Magn. Reson.* **2002**, *22*, 484−500.
(28) deAzevedo, E. R.; Tozoni, J. R.; Schmidt-Rohr, K.; Bonagamba, T. J. *J. Chem. Phys.* **2005**, *122*, 154506.
(29) Fujara, F.; Welfing, S.; Spiess, W. H. *J. Chem. Phys.* **1986**, *97*, 2928.

shift frequencies, which results from segmental reorientations that take place during a long (millisecond to second) mixing time (t_m). The quantification of the results obtained from the 1D PUREX experiments is usually done by the normalized pure-exchange intensity $E(t_m, \tau_{CSA}) = \Delta S/S_0$, which does not contain relaxation effects and just accounts for the signals of the reorienting segments. Information about motional correlation functions can be obtained by fitting the mixing time dependence of $E(t_m, \tau_{CSA})$ by a stretched exponential correlation function (also known as Kolrausch−William−Watts or KWW function[30]), with two fitting parameters, the mean correlation time and the stretching parameter β_{KWW}. The β_{KWW} values characterize the degree of non-exponentiality of the correlation function, being 1 for purely exponential correlation functions. Consequently, in the case of the heterogeneous scenario assumed in this work, it can be directly related to the width of the distribution of correlation times. However, for diffusive motions, such as in isotropic rotational diffusion, the distribution of reorientation angles β_R varies with the ratio t_m/τ_C, $R(\beta_R, t_m/\tau_C)$. Because of that, for isotropic rotational diffusion, non-exponential $E(t_m,\delta\tau_{CSA})$ versus t_m curves can be observed even for motions occurring with a single correlation time.[28] This can be understood considering that at smaller t_m/τ_C ratios, the peak in $R(\beta_R, t_m/\tau_C)$ occurs at small reorientation angles. As a result, the 1D PUREX experiment probes the early broadening of the peak near $\beta_R = 0°$. Afterward, because of the high sensitivity of this technique to small-angle motions, with $\beta_R \approx 10°$, the dephasing is complete for long evolution times τ_{CSA}. As a consequence, for long τ_{CSA}, the behavior of $E(t_m,\delta\tau_{CSA})$ as a function of t_m does not depend only on the correlation function of the motion but also on the t_m dependence of $R(\beta_R, t_m/\tau_C)$, as shown in refs 28 and 31. Thus, to quantify the distribution of correlation times unequivocally, it is necessary to measure the t_m dependence of $E(t_m,\delta\tau_{CSA})$ using different τ_{CSA} values,[19] which can significantly increase the measuring time, mainly for low abundant nuclei in non-labeled samples. Such an approach can be used to obtain the temperature dependence of the mean correlation time and the width of the distribution of correlation times. An alternative approach to achieving information about the distributions of correlation times (or on the non-exponentiality of the motional correlation functions in a more general picture) is measuring the temperature dependence of the $E(t_m,\delta\tau_{CSA})$ for fixed t_m and τ_{CSA}. The $E(t_m,\tau_{CSA})$ vs temperature T curves depend on the fraction of segments that move with rates within the time scale (dynamic window) that the exchange experiments are sensitive to (~100 μs to ~1 s). Thus, for thermally activated motions, occurring among M nonequivalent sites and with exponential correlation functions, there is a temperature at which all the molecular segments contribute to the observable exchange intensity. At this temperature, the $E(t_m, \tau_{CSA})$ vs T curve reaches a maximum value of $(1 - 1/M)$, which is ~1 for a large number of sites. In contrast, if the molecular reorientations occur with a distribution of correlation times, there is no temperature at which all molecular segments move simultaneously with rates within the dynamic window of the exchange experiment, and the maximum in the $E(t_m, \tau_{CSA})$ vs T curve is smaller than $(1 - 1/M)$. The larger is the width of the correlation time distribution, the smaller is the maximum of the $E(t_m, \tau_{CSA})$ vs T curve.[28] Because t_m and τ_{CSA} are fixed, the maximum of the $E(t_m, \tau_{CSA})$ vs T curve does not have a strong dependence of the distribution of reorientation angles $R(\beta_R, t_m/\tau_C)$, and for motions occurring between a large number of sites, it mostly depends on the width of the distribution of correlation times. The width of the $E(t_m, \tau_{CSA})$ vs T curve also depends on the distribution of correlation times, but it has an additional dependence on the thermal activation of the motion (Arrhenius or Williams−Landel−Ferry (WLF) processes and the corresponding parameters), so it is not a reliable parameter. Thus, with the presence of a distribution of correlation time, it is possible to estimate the width of such distribution from an $E(t_m, \tau_{CSA})$ vs T curve. However, there is a limiting feature if one needs a precise quantification. It is well-known that in many dynamic processes, including those related to the glass transition of amorphous polymers such polystyrene, polypropylene, and polyvinyl alcohol, the distribution of correlation times can vary significantly with temperature.[19,31] This can be incorporated in the simulation of the $E(t_m, \tau_{CSA})$ vs T curves, but would be hard to observe such behavior from a single $E(t_m, \tau_{CSA})$ vs T dependence. Thus, it is more convenient to simulate the curves considering a temperature-independent distribution of correlation times. The width of this temperature-independent distribution is not equal to the actual width of the temperature-dependent distribution of correlation times, but will depend on the degree of motional heterogeneity during the glass transition as well (in the sense of distribution of correlation times). This is so because the maximum mobile fraction seen in a PUREX experiment (maximum of the $E(t_m, \tau_{CSA})$ vs T curve) is proportional to the distribution of correlation times at the corresponding temperature. From now on the full width at half-maximum of the distribution of correlation times taken from the $E(t_m, \tau_{CSA})$ vs T curves will be referred to as $\langle\Delta\sigma\rangle$. Such an approach is obviously not as informative as the full characterization of the distribution of correlation times as a function of temperature by varying t_m and τ_{CSA}.[19] However, it still can be useful if one is not interested in the details of the distribution of correlation times, but just wants to know if some physical or chemical manipulations of the sample have an influence on it during a specific dynamic process. This is the case of the present work, in which the aim was to study the effects of Li^+ doping on the non-exponentiality of the correlation function of the slow motion in the ormolytes around the polymer glass transition.

^{7}Li Experiments. To measure the slow motion of the Li^+ cation in the ormolytes, the stimulated echo (STE) exchange experiment adapted for spin 3/2 systems was used. This recently developed experiment was first applied to study the slow exchange of the ^{7}Li and ^{9}Be cations in inorganic solid electrolytes.[26,27,32,33] The pulse sequence used in the experiment is shown in Figure 1c. Heteronuclear broad-band

(30) Williams, G.; Watts, D. C. *Trans. Faraday Soc.* **1970**, *66*, 80.
(31) Schaefer, D.; Spiess, H. W. *J. Chem. Phys.* **1992**, *97*, 7944−7953.
(32) Bohmer, R. *J. Magn. Reson.* **2000**, *147*, 78−88.
(33) Wilkening, M.; Heitjans, P. *Solid State Ionics* **2006**, 3031−3036.

decoupling was added into the original pulse sequence to eliminate the contribution of the Li−H interactions, which are strong for ormolytes.[9] Using the appropriate phase cycling and interpulse timing,[32] a stimulated echo with intensity $S(\tau,t_m,t) = \langle 9/20 M_0 \sin(\omega(0)\tau)\sin(\omega(t_m)\tau)\rangle$ is observed with a maximum at $t = t_m + 2\tau$. $\omega(t_m)$ represents the anisotropic NMR frequencies, resulting from quadrupolar or dipolar interactions, observed before and after the mixing time. The phase cycling and the interpulse time τ were chosen in order to enhance the quadrupolar contribution to the echo.[27,32] Because the quadrupolar frequency ω_Q depends on the strength and orientation of the electric field gradient at the cation site, any modification in these parameters changes this frequency. Thus, the experiment is sensitive to any exchange process that changes the electric field gradient around the Li^+-complexing sites ($-CH_2-\mathbf{O}-CH_2-$) of the polymer chain. The measurement of the stimulated echo amplitude as a function of the mixing time provides the correlation function of the exchange process. From these measurements, the mean correlation times (decay times) of the ionic motion can be obtained as a function of the temperature and, consequently, the activation energy. Longitudinal relaxation, T_1, also produces echo decay as a function of the mixing time, which may happen in the same time scale of the decay due to motion. Thus, to guarantee that only motion effects are encoded in the stimulated echoes, the data is normalized by the T_1 decay, which was estimated by an inversion recovery experiment. In fact, because T_1 was found to be much longer (the minimum observed was ~4 s) than the mixing time at all measured temperatures, such normalization had no effect on the data. In fact, because it is the term T_{20} that remains during t_m, the relevant relaxation time is T_{1Q}; however, this parameter is usually not so different from T_1, so we used T_1 for the correction. The normalization of the echo intensity by its value obtained at short mixing times performs the correction of T_2 relaxation effects during the period τ.

Experimental Section

Sample Preparation. The synthesis of Li^+-doped Type II ormolytes has already been detailed in refs 4−6. After the preparation and further drying to remove the solvents (vacuum heating), the nanocomposites were immediately sealed in appropriate sample tubes for NMR and aluminum pans for DSC experiments. The nomenclature used to describe the Type II composites is $[X]_n[y]$-II, where X represents the weight percent of polymer, n the polymerization degree, y the oxygen-to-lithium ratio, and II indicates that both ends of the polymer chains are chemically bonded to the siloxane structure.

Differential Scanning Calorimetry (DSC). The measurements were performed on 10 mg samples with a heating rate of 10 °C/min from −80 to 90 °C using a DSC−TA Instruments (model 2910). To determine the polymer glass-transition temperatures T_g, we used the middle point transition method indicated in Figure 3a.

NMR. The experiments were performed using a 9.4-T VARIAN INOVA spectrometer at ^{13}C, ^{7}Li, and ^{1}H frequencies of 100.5, 150.0, and 400.0 MHz, respectively. A 7 mm static double-resonance variable temperature Doty probe head was used. $\pi/2$ pulse lengths of 3.8 and 4.0 μs were applied for ^{13}C and ^{1}H, respectively. Proton decoupling field strength of approximately 60 kHz, cross-polarization time of 1.0 ms, and recycle delays ranging from 10 to 30 s were used. In 2D exchange experiments, 64−128 increments in t_1 were acquired using a total of 32 scans per t_1 point. The mixing times for 2D experiments were 200 ms. Hypercomplex acquisition was used to achieve a pure-absorptive 2D spectrum.[34] The 1D pure exchange NMR (1D PUREX) experiments were also performed using mixing times of 200 ms and τ_{CSA} of 1000 μs. ^{7}Li stimulated echo experiments were performed using pulse lengths of 4 μs, τ values of 10 and 20 μs, and t_m values ranging from 1 to 500 ms. The STE experiment was performed using a phase cycling that records only quadrupolar order during t_m. This phase cycling is described in ref 32.

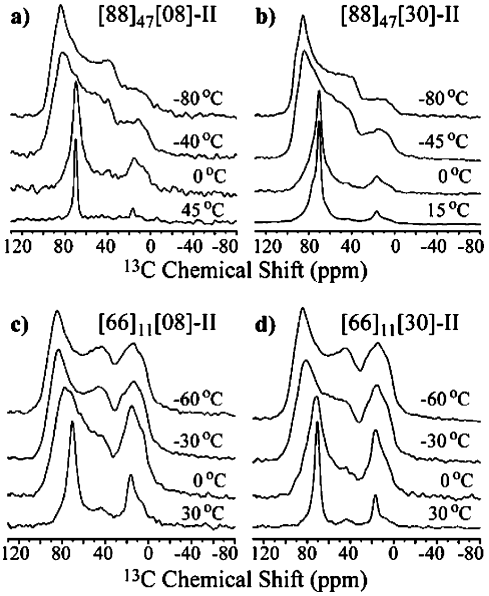

Figure 2. ^{13}C CP spectra of Type II Ormolytes as a function of temperature of samples: (a) $[88]_{47}[08]$-II, (b) $[88]_{47}[30]$-II, (c) $[66]_{11}[08]$-II, and (d) $[66]_1[30]$-II.

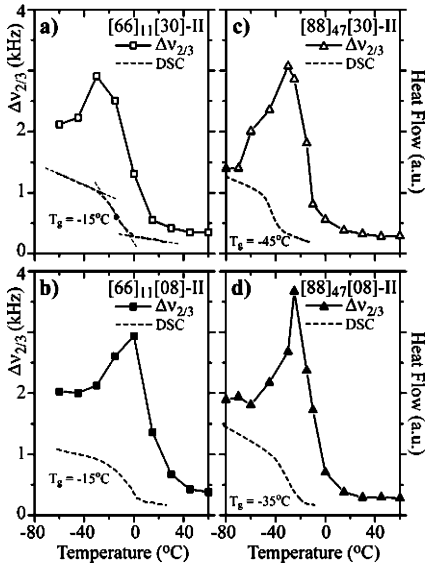

Figure 3. Line width at 2/3 of the maximum intensity measured as a function of temperature for Type II Ormolytes: (a) $[66]_{11}[30]$-II, (b) $[66]_{11}[8]$-II, (c) $[88]_{47}[30]$-II, and (d) $[88]_{47}[8]$-II.

Results

The possibility of observing separated ^{13}C chemical shift powder patterns in ormolytes makes it possible to study the

(34) States, D.; Haberkorn, R. A.; Ruben, J. *J. Magn. Reson.* **1982**, *48*, 286.

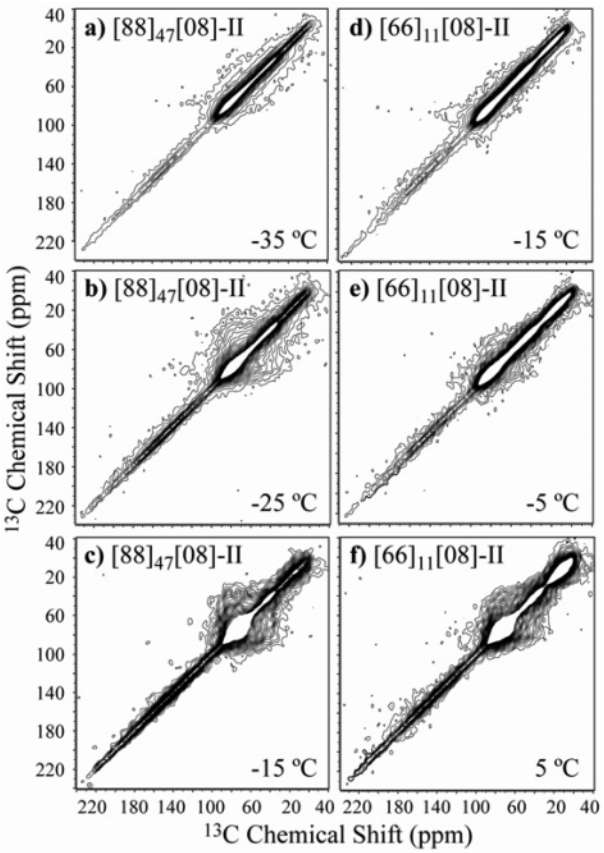

Figure 4. Two-dimensional exchange spectra for sample $[88]_{47}$[8]-II at (a) −35 °C (T_g), (b) −25 °C (T_g + 10 °C), and (c) −15 °C (T_g + 10 °C), and for sample $[66]_{11}$[8]-II at (d) −15 °C (T_g), (e) −5 °C (T_g + 10 °C), and (f) 5 °C (T_g + 20 °C). In all cases, 20 contour levels between 5 and 40% of the maximum intensity were used.

dynamics of the polymer chain by analyzing the spectral changes as a function of temperature. Figure 2 shows the line shape temperature dependence for Type II ormolytes. The spectral lines observed at the highest temperatures have already been assigned in ref 11. The resonances observed in the highest-temperature spectra around 15 ppm were assigned to the carbons belonging to CH_2 located in the linkage group [Si(**C**H_2)$_3$NHCONH(**C**H_2)$_3$]. The signal observed around 70 ppm is typical of carbons of [**C**H_2**C**H_2O] groups in PEO chains. In the rigid-lattice regime, at the lowest temperatures, a typical powder pattern spectrum for the carbons [**C**H_2**C**H_2O] is observed in the 35−100 ppm region. In this case, the chemical shift tensor parameters, σ_{xx} and σ_{yy}, for the [**C**H_2**C**H_2O] carbons can be obtained directly from the powder pattern, and σ_{zz} can be calculated using the isotropic chemical shift value taken from the high-temperature spectrum. Thus, the chemical shift tensor parameters for the [**C**H_2**C**H_2O] carbons become completely defined: $\sigma_{xx} = 93$ ppm, $\sigma_{yy} = 82$ ppm, and $\sigma_{zz} = 33$ ppm. With these identifications, the intensities observed within the 20 to −20 ppm spectral region can be attributed to **C**H_2 carbons belonging to the linkage group, which define the right-side shoulder observed in the powder spectrum at low temperatures. Additional intensities are observed in the spectral region above 100 ppm (not shown in Figure 2, but observed in Figure 4) can be attributed to the **C**O carbons also belonging to the linkage group.

The analysis of the ^{13}C line shapes versus temperature can provide information about molecular motion on the microsecond to millisecond time scale because of the orientation dependence of the chemical shift anisotropy (CSA).[15,23,35] This could be achieved by simulating the evolution of the ^{13}C magnetization belonging to different sites (different orientation of the molecules in respect to the B_0 field) under the influence of the molecular motions. However, this simulation has not been done in the case of heterogeneous systems such as ormolytes because the large distribution of motional rates and the complex motional geometries make it difficult to perform this calculation and extract motional parameters. Instead of simulating the spectra, we used the line width temperature dependence to estimate the temperature at which the motional narrowing starts. As the temperature increases, the molecular motion starts averaging the CSA interaction, producing a distortion in the powder spectrum, Figure 2. This distortion increases until featureless broad lines are obtained. At higher temperatures, the motional rate, $k \approx (\tau_c)^{-1}$, becomes larger than the full width of CSA, $\Delta\sigma = |\sigma_{xx} - \sigma_{zz}| = 60$ ppm ≈ 6 kHz, producing the complete averaging (fast exchange limit) of this interaction, Figure 2. The spectral shape in the fast limit regime reflects the averaging of the CSA tensor by the motion and, consequently, depends on the motional geometry. For isotropic motions, all three principal values are averaged out and a single isotropic line is observed in the fast exchange limit. This is the case observed in Figure 2, showing that the motion of the PEO units is mostly isotropic well above the polymer glass transition.

The motional narrowing is usually quantified by measuring the temperature dependence of the line width at half-maximum, $\Delta\upsilon_{1/2}$, or equivalently, the full width of the CSA, $\Delta\sigma$. However, the powder pattern distortion occurring around the onset of the motional narrowing cannot be observed by measuring $\Delta\upsilon_{1/2}$ or $\Delta\sigma$ versus temperature. On the other hand, taking the line width at two-thirds of the maximum height, $\Delta\upsilon_{2/3}$, an initial broadening precedes the motional narrowing peaking in a well-defined temperature, which reflects the powder pattern distortion due to motions occurring with rates on the order of kHz.[15,36] In the case of ormolytes, the line narrowing is associated with the increase in chain motion that occurs close to the polymer glass-transition temperature, T_g, as already observed from DSC and ^{7}Li, ^{13}C, and ^{1}H line width measurements as a function of temperature in references 4−6 and 9−11. Figure 3 shows the temperature dependence of $\Delta\upsilon_{2/3}$ for Li^+-doped Type II ormolytes together with the respective DSC traces shown with arbitrary units. The maximum of the $\Delta\upsilon_{2/3}$ vs T curves fairly coincides with middle point transitions of the DSC curves.[9] The glass-transition temperatures found from the DSC curves for the samples $[66]_{11}$[8]-II, $[66]_{11}$[30]-II, $[88]_{47}$-[8]-II, and $[88]_{47}$[30]-II, were -15 ± 2, -15 ± 2, -35 ± 2, and -45 ± 2 °C, respectively.

(35) Spiess, H. W. In *NMR Basic Principles and Progress*; Diehl, P., Fluck, E., Kosfield, R., Eds.; Springer Verlag: Berlin,1978; Vol. 15, p 55.
(36) deAzevedo, E. R.; Bonagamba, T. J.; Reichert, D. *Prog. Nucl. Magn. Reson. Spectrosc.* **2005**, *47*, 137−164.

Comparing molecular motions in different samples is difficult because they may vary with temperature. This means that it is not important to compare the samples at the same temperature, but in situations in which the motional regimes are similar. This can be done by choosing the temperature for performing the experiments according to a reference temperature that must be directly related to the molecular motional rate.

Figures 4a−c show the experimental 2D exchange spectra acquired with t_m = 200 ms for the sample $[88]_{47}$[8]-II at −35 °C (T_g), −25 °C (T_g + 10 °C), and −15 °C (T_g + 20 °C). The temperatures were chosen to cover the range in which the motions occur in the slow-motion regime. The 2D spectrum obtained at −25 °C clearly shows two distinct regions. The first spectral region attributed to the ^{13}C nuclei in the linkage groups (below 35 and above 100 ppm) is fully diagonal. The prominent diagonal signal observed above 100 ppm is attributed to the CO group in the linker, which did not appear in the high-temperature spectra due to the loss of cross-polarization efficiency. The second spectral region (between 35 and 100 ppm), associated with the signal from the $[CH_2CH_2O]$ groups, is typical for segments executing isotropic motion. In summary, basically the same behavior was observed for non-doped Type II ormolytes in ref 11. At −15 °C, it is possible to observe that the signal for the carbons belonging to the linker also shows some non-diagonal intensity, but it is still much closer to the diagonal than the signal for the $[CH_2CH_2O]$ groups. This confirms that the hindrance to the molecular motion of the groups close to the silica structures might be effective even for higher temperatures, as already observed for non-doped samples.[11]

Figures 4d−f show the 2D exchange spectra acquired with t_m = 200 ms for the sample with approximately 4 times shorter PEO chain $[66]_{11}$[8]-II at −15 °C (T_g), −5 °C (T_g + 10 °C), and 5 °C (T_g + 20 °C). In this case, the differences between the 2D patterns from the linker and $[CH_2CH_2O]$ groups are less pronounced. Actually, this difference is clearly observed at 5 °C, which suggests that the effect of the silica structure on hindering the molecular motion extends for all polymer chains as also observed for non-doped Type II ormolytes,[11] this effect being more pronounced for shorter PEO chains. However, the difference in the spectral patterns for different temperatures is considerable.

Figure 5 shows the $E(t_m,\delta\tau_{CSA})$ intensities vs temperature, acquired with t_m = 200 ms and τ_{CSA} = 500 μs. The measurements were performed for samples $[88]_{47}[\infty]$-II (non-doped), $[88]_{47}$[08]-II, and $[88]_{47}$[30]-II. It can be noticed that the measurements were performed only in the low-temperature side of the curve. This is due to the fact that the intensity of the reference 1D PUREX spectrum S_0 (0, $\delta\tau_{CSA}$) is drastically reduced by dynamics occurring with rates on the order of a few kilohertz (intermediate regime) during the evolution period τ_{CSA}, in which the motion-induced chemical-shift frequency changes prevent the formation of a full stimulated echo. As a result of this intensity reduction, the sensitivity of the experiment in the intermediate exchange regime is decreased. In conjunction with the line broadening induced by the interference of the motion with proton

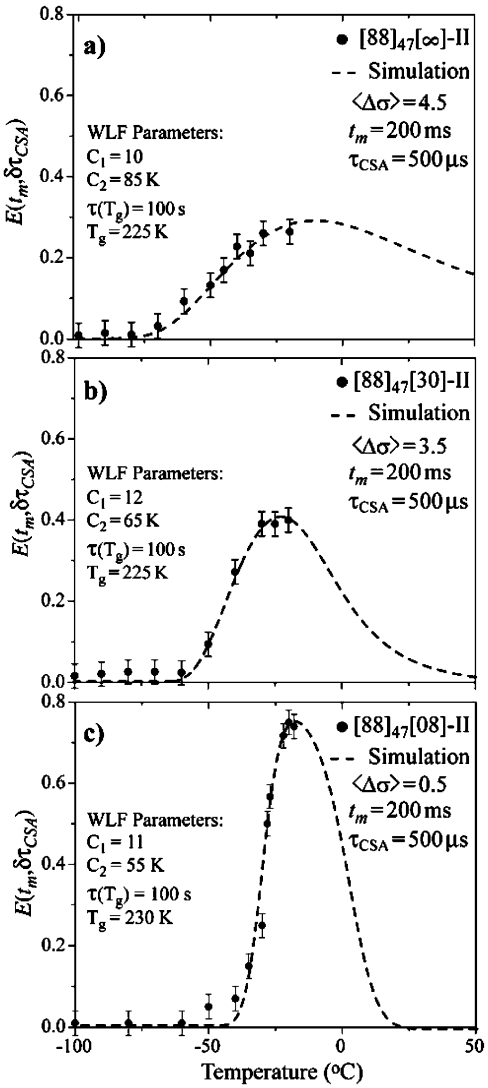

Figure 5. Experimental and simulated 1D PUREX intensities $E(t_m,\delta\tau_{CSA})$ vs temperature for Ormolyte samples with different Li^+ doping levels. The WLF parameters used in the simulation are shown.

decoupling,[36,37] this precludes the acquisition of $E(t_m,\delta\tau_{CSA})$ vs T data in the intermediate-motion regime. Nevertheless, it is observed that, although the maximum intensities of the $E(t_m,\delta\tau_{CSA})$ vs T curves increase as a function of the Li^+ doping level, their widths decrease with this parameter. Because the width of the distribution of correlation times is inversely proportional to the maximum intensity of the $E(t_m,\delta\tau_{CSA})$ vs T curve, this shows that the Li^+ doping decreases the distribution of correlation times of the polymer chains dynamics. To confirm such behavior, we simulated the $E(t_m,\delta\tau_{CSA})$ vs T curve. For that, some geometry for the molecular motion must be assumed. Such a model can be inferred from previous works in which the molecular dynamics of various amorphous polymers were studied in detail around the glass transition by using 1D, 2D, and 3D exchange NMR experiments.[19,38,39] Particularly, in some references,[19,38,39] it has been shown that the geometry of the

(37) Takegoshi, K.; Hikichi, K. *J. Chem. Phys.* **1991**, *94*, 3200.
(38) Leisen, J.; Schmidt-Rohr, K.; Spiess, H. W. *J. Non-Cryst. Solids* **1994**, *172*, 737−750.
(39) Heuer, A.; Leisen, J.; Kuebler, S. C.; Spiess, H. W. *J. Chem. Phys.* **1996**, *105*, 7088−7096.

motion around the glass transition is composed of small-angle step isotropic rotational diffusion accompanied by large-angle jumps due to conformational transitions. It has also been found that both processes occur with a distribution of correlation times. Following the discussion on the NMR background section and in ref 38, it was assumed that the distribution of correlation times for the conformational jumps and the small-angle diffusion was the same and temperature independent. Given that the intention of this work is to probe overall the modifications in the distribution of correlation times of the slow motion in the ormolytes around the polymer glass transition upon Li^+ doping, this assumption is appropriate. However, it is not possible to either quantify the distribution of correlation times at different temperatures or separate the behavior of the conformational jump and diffusive motions. The resulting simulations and the corresponding $\langle\Delta\sigma\rangle$ of the log-Gaussian distribution of correlation times (in decades) are also shown in Figure 5. It can be observed that $\langle\Delta\sigma\rangle$ clearly tends to decrease for increasing Li^+ doping levels. Note that for the non-doped sample, $\langle\Delta\sigma\rangle \approx 5$ decades. This may look inconsistent with the powder pattern at room temperature shown in ref 11. For such a large distribution of correlation times, the room-temperature spectrum should present at least two distinguishable components, a Lorentzian line associated with segments that move with correlation times short enough to average out the CSA and a powder pattern associated with those segments that moves within the slow-motion regime. Instead of that, a single sharp line is observed, showing that at room temperature, the distribution of correlation times is sharp enough to have most of the segments in the fast motion regime. This actually shows that the $\langle\Delta\sigma\rangle$ obtained from the 1D PUREX experiments does not describe the full behavior of the distribution of correlation times, which tends to decrease as a function of temperature. However, in ref 28, $E(t_m,\delta\tau_{CSA})$ vs T curves were measured for two very well characterized samples, atactic polypropylene (aPP), for which the glass transition takes place with a large distribution of correlation times (~4 decades), and polyisobutylene (PIB), for which the glass transition occurs with a small distribution of correlation times (<1 decade). The same behavior for the $E(t_m,\delta\tau_{CSA})$ vs T curves is observed here, confirming that the decrease of $\langle\Delta\sigma\rangle$ upon Li^+ doping can be associated with the non-exponentiality of the correlation function. Another feature of such simulations is that to produce the correlation time−temperature correspondence, one needs to assume a model that gives the thermal activation of the motion. However, note that the maximum reached by the $E(t_m,\delta\tau_{CSA})$ vs T curve is independent of these models, i.e., the choice of activation model does not influence the above discussion. Because we are dealing with dynamics around the glass transition, the most appropriate function is a nonlinear temperature dependence of the correlation time, such a WLF equation.[40] For all samples, the fittings are slightly better if the simulations are performed using the WLF equation instead of assuming an Arrhenius behavior with the activation energy and τ_0 with physically meaningful values. Additionally, the WLF parameters used in the simulations of the $E(t_m,\delta\tau_{CSA})$ vs T curves are pretty much in the typical range found for the glass transition of amorphous polymers.[23,31]

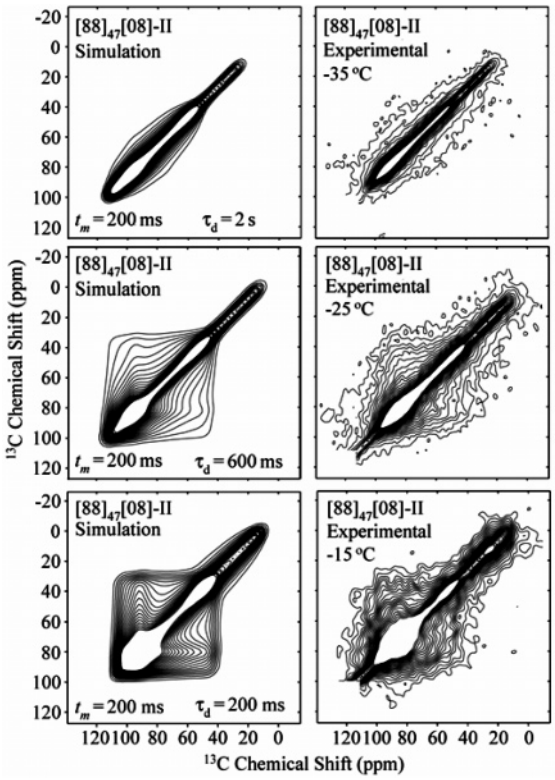

Figure 6. Simulated and experimental 2D exchange spectra for sample $[88]_{47}$[8]-II at −35 °C (T_g), −25 °C (T_g + 10 °C), and −15 °C (T_g + 20 °C). These simulations were performed using the slow motion approach with a short time cutoff of 500 μs.

To support these results, the PEO portion of the 2D exchange NMR spectrum of the sample $[88]_{47}$[08]-II was simulated using isotropic rotational diffusion and a log-Gaussian distribution of correlation times with width of 0.5 decade. A model that assumes a combination of small-angle motions, taken into account using small step isotropic rotational diffusion, and large-angle jumps, taken into account using random jumps, was used in the simulation. Because both motions occur simultaneously, it was also assumed that the correlation time of the jumps and the diffusion time of the isotropic rotational diffusion are the same. The mean correlation times of the diffusive process τ_d are indicated in Figure 6 and follow the same behavior as the one used in the simulations of the $E(t_m, \delta\tau_{CSA})$ vs T curves. The results for the temperatures −35 °C (T_g), −25 °C (T_g + 10 °C), and −15 °C (T_g + 20 °C) are shown in Figure 6. The agreement between the experimental and simulated spectra is fairly good.

To provide a better understanding about the relationship between the cation motion and the chain dynamics in Li^+-doped ormolytes, it is also important to study the Li^+ motion as a function of temperature and compare the results with those obtained for the polymer chain dynamics. This has been extensively done for solid polymer electrolytes by solid-state NMR, mostly using ^7Li and ^1H relaxation experiments and

(40) McCrum, N. G.; Read, B. E.; Williams, G. *Anelastic and Dielectric Effects in Polymeric Solids*, 2nd ed.; Dover: New York, 1991; Vol. 1.

line width analysis.[9,41] To correlate the slow chain dynamics, studied by 2D exchange and 1D PUREX NMR, with the slow cation motion, ^{7}Li stimulated echo experiments were carried out for the sample $[88]_{47}$[08]-II. As usual in inorganic ionic conductors, because the local electric charge distribution in the vicinity of the ion is different at distinct sites, the electric field gradient may vary from site to site. As a consequence, the ions experience different quadrupolar frequencies as they move through these electrically nonequivalent sites, making possible to detect the cation translational motion in the STE experiments. In solid polymer electrolytes, the polymer dynamics by itself can also change the local electric field gradient in the vicinity of the cation, affecting as well the stimulated echo amplitude. Thus, it is difficult to distinguish whether the decay of the stimulated echo amplitude comes from the cation hopping or from the modulation of the electric filed gradient by the polymer dynamics. On the basis of previous studies that show that the motional narrowing of the ^{1}H and ^{13}C lines occurs at temperatures ~20 °C below the narrowing of the ^{7}Li line associated with the central transition,[9] one can infer that both processes, polymer and lithium motions, occur on the sample in almost the same temperature range. Besides, a significant narrowing of the central lithium line occurs even under high-power ^{1}H decoupling, which indicates that there is some lithium motion independent of the chain dynamics.[9,41] Figure 7a shows a comparison between ^{7}Li spectra for the samples $[88]_{47}$[08]-II obtained with the standard quadrupolar echo and the stimulated echo pulse sequence with $\tau = 20\ \mu$s. Both the quadrupolar and dipolar contributions can be refocused simultaneously by the stimulated echo; however, they can be separated by the appropriate choice of the evolution time τ, because the typical decay times are very different for these interactions ($1/\delta_D - 15/\delta_Q$). Thus, because of the short $\tau = 20\ \mu$s value used in the stimulated echo sequence, the respective spectra are predominately due to the quadrupolar interaction. To ensure such statement, we performed a set of experiments. In these experiments, the echo amplitudes were measured as a function of τ at the echo maximum, $S(\tau,t_m,\tau)$, and $t_s = 64\ \mu$s later, $S(\tau,t_m,\tau + t_s)$. The results are shown in Figure 7b. Because the echo due to the dipolar contribution decays much slower than the quadrupolar one, the intensity at the echo maximum $S(\tau,t_m,\tau)$ is mostly due to the latter interaction. In contrast, for $S(\tau,t_m,\tau + t_s)$, the echo due to the quadrupolar order has already decayed and the echo intensity is due to only the dipolar contribution. Figure 7b shows that the intensity at the maximum of the stimulated echo at short echo times is essentially produced by the quadrupolar interaction for all temperatures.

Figure 8a shows the t_m dependence of $S(\tau,t_m,\tau)$ curves obtained with $\tau = 20\ \mu$s at different temperatures for sample $[88]_{47}$[08]-II. In the case of long mixing times, ^{1}H-driven ^{7}Li spin-diffusion can be very effective as an exchange mechanism, which can interfere within the interpretation of the decay curves in terms of molecular motion. Thus, all the curves shown in Figure 8 were normalized by the decay

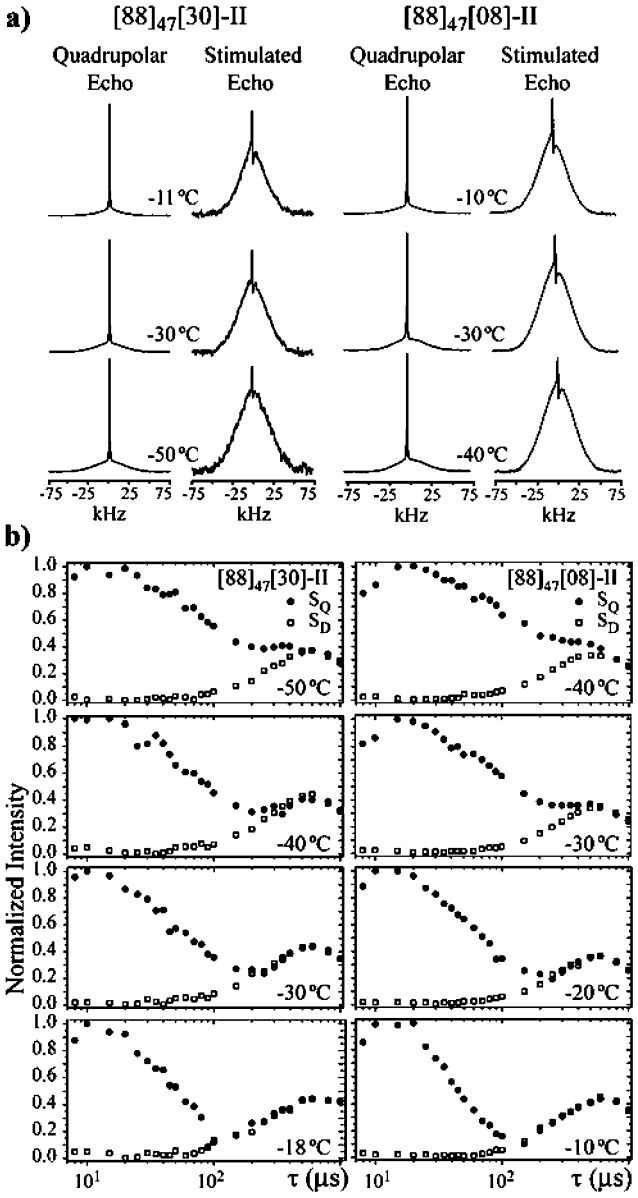

Figure 7. (a) ^{7}Li quadrupolar and ^{7}Li Stimulated echo spectra of samples $[88]_{47}$[30]-II and $[88]_{47}$[8]-II at selected temperatures. The spectra are scaled such that they exhibit the same maximum intensities. (b) ^{7}Li stimulated echo amplitude as a function of τ, at selected temperatures, for samples $[88]_{47}$[30]-II and $[88]_{47}$[8]-II. The amplitudes were measured at the echo maximum, $S(\tau,t_m,\tau)$ (●), and $t_s = 64\ \mu$s later, $S(\tau,t_m,\tau + t_s)$ (□).

due to spin-diffusion, which was obtained from a measurement at low temperature (−60 °C). This refers to the standard correction of the data to the spin diffusion, which relies on measuring the stimulated echo at low temperature, fitting the curves by the appropriate correlation function, and normalizing the high-temperature data by this decay. This obviously supposes that the spin diffusion process is temperature independent, which is indeed a good approximation in the reduced temperature range of the measurements. After this normalization, the $S(\tau,t_m,\tau)$ vs t_m curves at each temperature were fitted by the KWW function, providing the temperature dependence of the correlation times, Figure 8b. The curvature observed in the Arrhenius plot of Figure 8b is probably due to spin diffusion processes at long mixing times, which were not compensated by the normalization and affecting the correlation times at low temperatures. Despite

(41) Donoso, J. P.; Bonagamba, T. J.; Panepucci, H. C.; Oliveira, L. N.; Gorecki, W.; Berthier, C.; Armand, M. *J. Chem. Phys.* **1993**, *98*, 10026−10036.

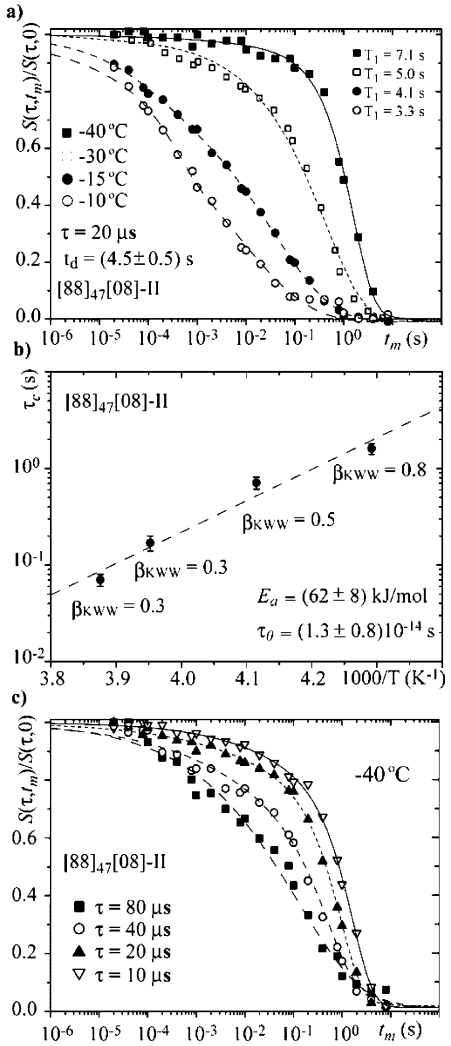

Figure 8. ^{7}Li stimulated echo amplitudes $S(\tau,t_m,\tau)$: (a) t_m dependence for sample [88]$_{47}$[08]-II at four different temperatures. The lines are KWW fittings corrected by the spin diffusion effects represented by an exponential decay time constant of 4.7 s, as indicated by t_d in the figure. (b) Arrhenius plot from the correlation times extracted from part a. The β_{KWW} values at each temperature are also shown in the figure. (c) $S(\tau,t_m,\tau)$ vs t_m at different τ values for the sample [88]$_{47}$[08]-II at $T = -40$ °C.

the expected behavior for these curves not being an Arrhenius law, it may appear as a linear dependence because of the small frequency range that the exchange experiment is sensitive to. In this sense, the linear fit presented in Figure 8b may provide only an apparent activation energy, which can be estimated as (62 ± 8) kJ/mol. The intensity of the stimulated echo at long mixing times is related to the number of sites involved in the motion. In this case, the intensity is mostly zero, which shows that the detected Li exchange involves occur between many (theoretically infinity) electrically nonequivalent sites. Actually, for this kind of materials, for which the polymer chains are mostly amorphous, the presence of many nonequivalent complexing sites is expected, in contrast to the case of crystalline electrolytes, for which there is a limited number of nonequivalent sites. Besides that, the modulation of the electric field gradient by the chain motion, which also affects the detected exchange intensity, also has a diffusive character. This is confirmed by the $S(\tau,t_m,\tau)$ vs t_m curves measured with different τ values shown in Figure 8c, where it can be noticed that the decay

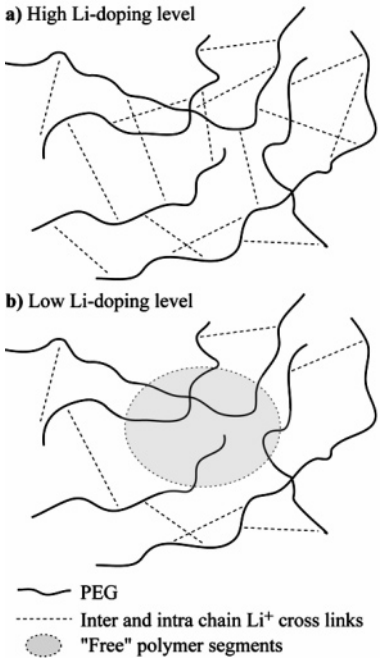

Figure 9. Sketch of the model used to explain the dependence of the motional heterogeneities on the Li doping levels. The siloxane structure is not shown in this sketch.

constant depends on τ. Such behavior is expected if the mobile nucleus experiences many but only slightly different electric field gradients.[27,28,42] In addition to that, the β_{KWW} value is quite small for all temperatures, showing that the ^{7}Li Exchange curves are considerably affected by the micro heterogeneity of the cation environment.

Discussion

The main interesting finding of this work is related to the decrease in the non-exponentiality of the correlation function that describes the chain dynamics around the glass-transition temperature upon Li^+ doping. Assuming that such non-exponentiality is due to a distribution of correlation times, it is possible to propose a model that can explain this behavior, Figure 9. At high doping levels, the Li^+ cation can make intra- or interchain cross-links between polymer segments, producing a dense network of cross-linked polymer, Figure 9a. When thermal energy is supplied to the sample, the weak O···Li cross-links can be broken and the "free" polymer segments enhance their molecular motions. At high Li^+-doping levels, many polymer segments are involved in the complexation of the Li^+, which increases the glass transition of the polymer chain and reduces the Li mobility.[9] On the other hand, once the O···Li links are broken by the thermal energy, all the polymer segments start moving together, resulting in the uniformization of the molecular motions responsible for the onset of glass transition, which then occur with a small distribution of correlation times. On the contrary, at lower doping levels, the number of cross-linked sites is smaller and, as a result, the presence of "free" polymer segments (that do not form complexation sites) is more probable (Figure 9b). Thus, many of the polymer chains

(42) Bohmer, R.; Diezemann, D.; Hinze, G.; Rossler, E. *Prog. Nucl. Magn. Reson. Spectrosc.* **2001**, *39*, 191.

will behave as "non-doped" chains and will experience the natural environment microheterogeneities of glassy systems, leading to a glass transition with a broad distribution of correlation times.[16,17] Therefore, our results suggest that Li^+ doping modifies the local interactions between the polymer segments in such a way that the characteristic distribution of correlation times of the motions that occurs around the glass transition temperature are minimized. Thus, it is an indication that besides being the charger carrier, the Li^+ ions act as cross-linkers, changing the dynamic behavior of the polymer chains.

Another important question that could be addressed is whether the cations Li^+ are preferentially dissolved by isolated PEO chains, intrachain cross-linking, or make cross-links between different chains, interchain cross-linking. Unfortunately, our results cannot unambiguously answer this question because either the increase of the glass transition or the decrease in the distribution of correlation times upon Li^+ doping is in agreement with both cases. This can be understood considering that the distribution of correlation times of the motion occurring around the glass transition is usually associated with heterogeneities in the molecular environment.[16,18,43] Thus, because either the presence of ions dissolved by isolated PEO chains or making cross-links between chains are expected to produce a more homogeneous environment (different chains tend to have similar dynamic behavior), both hypothesis would be in agreement with our results.

Some studies on polymer electrolytes have also shown the effects of Li^+ doping on the polymer dynamics, indicating that the heterogeneity of the segmental motions is affected by the presence of Li^+ ions (*44*,*45*).

Conclusions

^7Li and ^{13}C solid-state NMR methods were used to study Li^+-doped siloxane/poly(ethylene oxide) hybrid ionic conducting materials, where the polymer chains interact with the inorganic phase through covalent bonds. The effect of the interactions between the organic and inorganic phases (siloxane and lithium) on the polymer dynamics was analyzed. The motion geometry of polymer chains was found to be similar for doped and non-doped hybrids. Although the motion of polymer segments near the linkage groups is very hindered by the urea linkages to the siloxane structures, the motion of segments away from these structures follows the dynamic behavior expected for amorphous polymers around the glass-transition temperature. It was also observed that at temperatures around the glass-transition, the non-exponentiality of the correlation function that describes the polymer chain dynamics is reduced upon Li^+ doping. Such behavior was explained considering that this non-exponentiality is associated with a distribution of correlation times. The Li^+ doping modifies the local interactions between the polymer segments reducing the distribution of correlation times of the motions responsible by the glass transition.

Acknowledgment. The Brazilian Science Foundation Agencies FAPESP, CNPq, and CAPES supported this research.

CM060762E

(43) Tracht, U.; Wilhelm, M.; Heuer, A.; Spiess, H. W. *J. Magn. Reson.* **1999**, *140*, 460−470.

(44) Vogel, M.; Torbrügge, T. *J. Chem. Phys.* **2006**, *125*, 054905.

(45) Vogel, M.; Torbrügge, T. *J. Chem. Phys.* **2006**, *125*, 164910.